UKRAINIAN CATHOLIC UNIVERSITY

BACHELOR THESIS

Causal brain activity modeling for the understanding of epilepsy pathogenesis

Author:
Sofiya GARKOT

Supervisor:
Moritz
GROSSE-WENTRUP

A thesis submitted in fulfillment of the requirements for the degree of Bachelor of Science

in the

Department of Computer Sciences
Faculty of Applied Sciences


УКРАЇНСЬКИЙ КАТОЛИЦЬКИЙ УНІВЕРСИТЕТ
APPLIED
SCIENCES
FACULTY

Lviv 2022

Declaration of Authorship

I, Sofiya GARKOT, declare that this thesis titled, "Causal brain activity modeling for the understanding of epilepsy pathogenesis" and the work presented in it are my own. I confirm that:

- This work was done wholly or mainly while in candidature for a research degree at this University.
- Where any part of this thesis has previously been submitted for a degree or any other qualification at this University or any other institution, this has been clearly stated.
- Where I have consulted the published work of others, this is always clearly attributed.
- Where I have quoted from the work of others, the source is always given. With the exception of such quotations, this thesis is entirely my own work.
- I have acknowledged all main sources of help.
- Where the thesis is based on work done by myself jointly with others, I have made clear exactly what was done by others and what I have contributed myself.

Signed:

Date:

UKRAINIAN CATHOLIC UNIVERSITY

Faculty of Applied Sciences

Bachelor of Science

Causal brain activity modeling for the understanding of epilepsy pathogenesis

by Sofiya GARKOT

Abstract

Epilepsy affects 1% of the world's population yearly and is one of the most widespread diseases. Although some forms of epilepsy are effectively treated using a medication, nearly every third patient needs surgical intervention to remove the epileptogenic area.

This study examined an epileptic brain's activity during the hallmarks of epileptic activity - interictal epileptiform discharges (IEDs) - using Causal Bayesian Networks. Results showed that trends of causal activity increase before an IED and decrease afterwards, differentiating across awareness states. Another benefit of the study is the recommendation system for a clinician while evaluating the epileptogenic region. The channels that have most frequently been a cause of an IED are reported as a potential resection area.

The code is freely available on the Github repository with the corresponding documentation for a clinician.

Acknowledgements

First and foremost, I would like to thank my thesis advisor, Moritz Grosse-Wentrup, who suggested the topic, provided clear explanations, ensured understanding, and cared about me during the most challenging times.

I also want to deeply thank the clinician Johannes Lang, who was available anytime to provide a medical perspective to the study.

A particular place in my heart is dedicated to the Machine Learning Lab at Ukrainian Catholic University, enhancing science at our university and preparing leading ML researchers.

Without the Applied Science Faculty, I would literally never started the journey as a programmer, and I would not finish this four-year-journey without my friends and family. Thank you for support!

Last but not least, I would like to express my gratitude to the Armed Forces of Ukraine - thus, I can defend my thesis in Ukraine.

Contents

List of Figures

List of Tables

List of Abbreviations

IED	**I**nterictal **E**pileptiform **D**ischarges
ECoG	**E**lectro**C**ortico**G**raphy
iEEG	**i**ntracranial **E**lectro**E**ncephalo**G**raphy
SEEG	**S**tereotactic **E**lectro**E**ncephalo**G**raphy
ASM	**A**nti **S**eizure**M**edication

To the bravest of the Earth - to Ukrainians

Chapter 1

Introduction

According to the World Health Organization (WHO, 2022), epilepsy affects 50 million people worldwide. The main symptom of epilepsy is seizures. Seizures involve sudden, temporary bursts of electrical activity in the brain that change or disrupt the way messages are sent between brain cells. These electrical bursts cause involuntary changes in body movement, function, sensation, behavior, or awareness (Kiriakopoulos, 2019). Seizures can also be accompanied by the loss of consciousness and control of bowel or bladder function. Epilepsy is defined as having two or more unprovoked seizures occurring more than 24 hours apart.

Epilepsy treatment varies depending on the form and a patient's state. The most wide-spread way of epilepsy treatment is anti-seizure medications (ASM). However, studies (Picot et al., 2008) show that nearly a quarter of patients with seizures have a drug-resistant form of epilepsy. Thus, the recommended therapy is epilepsy surgery. An evaluation for epilepsy surgery is appropriate for patients with seizures that may be focal in origin and continue to occur despite treatment with ASM. Although usually seen as the last option, the invasive treatment shows significant improvement in the patient's quality of life and seizure frequency when performed in the early stages after diagnosing drug-resistance (Engel et al., 2012). Thus, quick presurgical analysis is of great importance.

The effectiveness of epilepsy surgery is more significant than that of the ASM: around 70% of people who have temporal lobe surgery find that the surgery stops their seizures, and they become seizure-free. For a further 20% of patients the seizures are reduced (Epilepsy, 2021).

Before the surgical therapy, a doctor carefully evaluates the patient's clinical history. The reasoning for surgical intervention is based on the presumption that seizures can be abated if the critical mass of the epileptogenic network is safely removed or disconnected. For the evaluation of the epileptogenic zone (EZ), a subject undergoes previous monitoring using video-EEG, a variety of tests, and intracranial EEG observation. It may take up to a month of invasive recording before a doctor will come up with conclusions about the exact location of the EZ.

There are two distinct phases in epilepsy: ictal corresponding to the period of seizures and interictal corresponding to the period between them. During the interictal period a brain generates abnormal activity, namely interictal epileptiform discharges (IEDs).

In order to evaluate the epileptogenic region, the smaller units of epileptic activity - the IEDs - are later tracked on the recorded iEEG by a clinician. Based on the evidence, the region of surgical intervention is determined, and the operation is performed.

Generally, there are two types of invasive brain monitoring: Electrocorticography (EcOG) and Stereotactic-electroencephalography (SEEG). While EcOG can cover a selected brain area more densely, SEEG electrodes are deeper than EcOG, enabling the monitoring closer to the source of epileptic activity.

The sample SEEG setup in the case of patient №8 is visible in Figure 1.1, and cortical reconstruction from MRI is in Figure 1.2.

Problem statement

Since epilepsy is a dynamic disorder of the brain, it is particularly interesting to study it from a computer modeling perspective.

The first problem is the question of an IED formation: does the epileptic activity differ before and after a discharge and across the different awareness states. The developed computer model will provide more evidence for epilepsy pathogenesis, answering the question of how IEDs form.

As a result of the cause-effect modeling, the source region of discharges can be estimated. Thus, another challenge is an assistant model for a clinician that will point to the source of discharges.

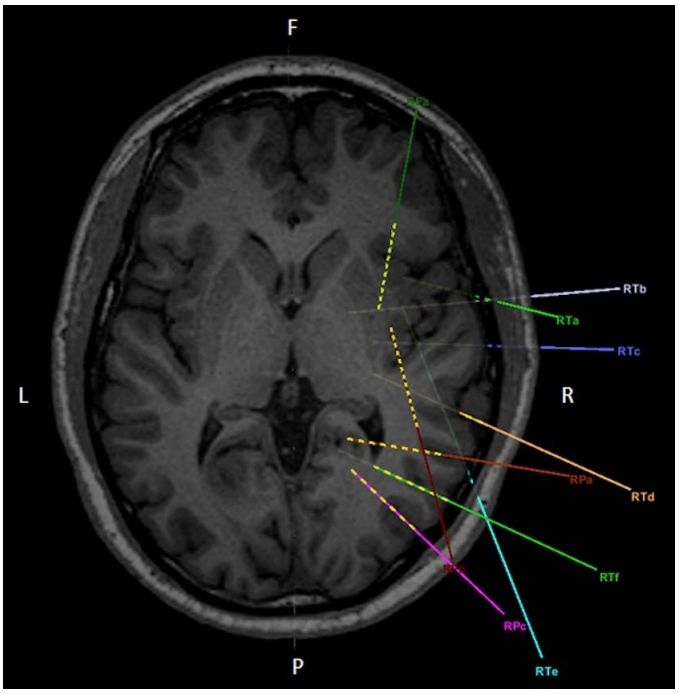

FIGURE 1.1: MRI-based 3D scheme of SEEG implantation: patient №8.

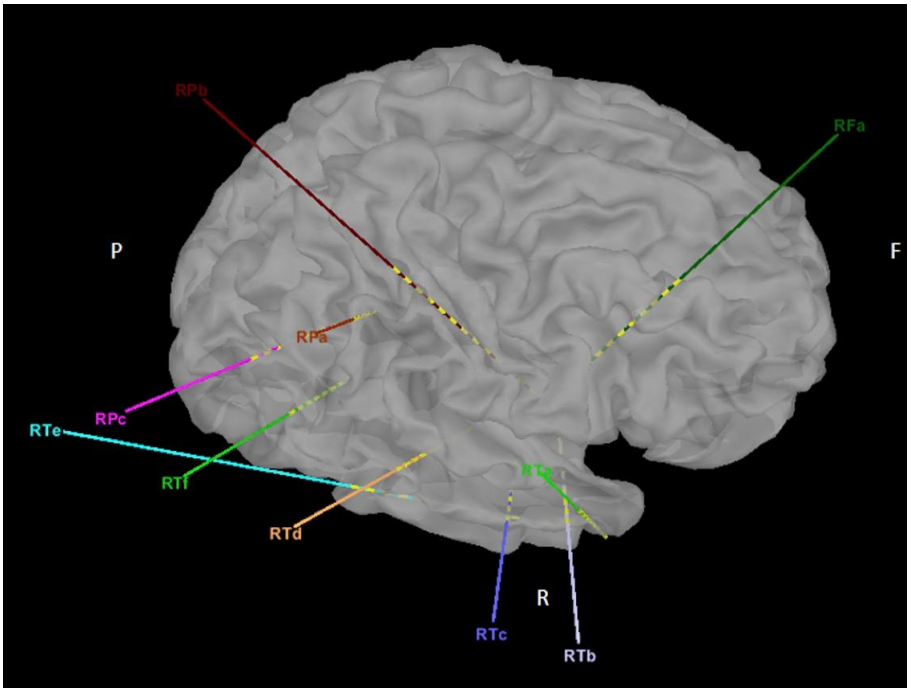

FIGURE 1.2: Cortical reconstruction from MRI of the patient №8.

Chapter 2

Literature review

IEDs and epilepsy

The electrical brain activity, recorded by iEEG, consists of rhythmic components. These components reflects neural oscillations, which are fluctuations in the populations of neurons (Cohen, 2014). Brain rhythms can be distinguished into five bands based on the frequency of oscillations.

1. Delta band (2 to 4 Hz) are registered during deep sleep, trance or coma.
2. Theta band (4 to 8 Hz) are present during deep relaxation, sleep, or meditation.
3. Alpha band (8 to 12 Hz) is registered in a person awake with eyes closed.
4. Beta band (15 to 30 Hz) are detectable in the awake state of a person.
5. Gamma band (>80 Hz) are registered during high cognitive processes.

Interictal epileptiform discharges are high-frequency oscillations lasting less than 80 milliseconds during the period between two consecutive ictal onsets. The studies of seizure origins showed their relation to IEDs: they may originate from a complex interaction between separate brain regions, and the correct detection and resection of IED-leading areas improves seizure control and reduce neurological, neuropsychological, and psychiatric post-surgical morbidity (Alarcon et al., 1997, Qi et al., 2020) .

There are several dysfunctional regions in epileptic patients: the irritative zone (IZ) - responsible for IEDs generation and the seizure onset zone (SOZ) - region, where the first electrophysiological changes are detected at ictal onset (Amini et al., 2011). The relationship between these regions (IZ and SOZ) has been a subject of debate. The very early study in this domain (Gotman, 1991) shows the dissociation between spikes and seizures and doubts medication's direct influence on spiking. In contrast, a more recent study by Azeem et al., 2021 shows the opposite. The authors modeled an epileptic network based on interictal spike propagation in the form of a graph. A brain state at a particular electrode represented a node in a graph and was correspondingly classified into a source, intermediate and terminal. The class was prescribed depending on whether spikes were starting, ending, or both coming and outgoing from a particular channel. The results showed that the resection of an

area including at least two such source nodes would result in a 70% reduction of spike propagation, supporting the connection between the IEDs and the onsets decrease. Similar were the results of Bartolomei et al., 2016: including the regions with high spike rate is associated with good post-surgical outcome.

Causal activity modeling of a brain

One of the central tasks in neuroimaging is modeling the brain's connectivity (Health NIH, 2009). Connectivity is defined as the estimation of interactions and communication between distinct units of the central nervous system and is subject to inputs producing outputs (Friston, 2003). The causal relationships of different brain regions are one of the key problems in the domain. That is why most of the discussed methods of estimating causal relationships arose from studies on connectivity.

There are several ways of modeling causal brain activity: Causal Bayesian Networks (CBN) (Grosse-Wentrup et al., 2015), Dynamic Causal Models (DCM) (Friston, 2003), Hierarchical Dynamic Models (Friston, 2008), Directed Markov Graphical Models (Biswas and Shlizerman, 2022), Structural Equation Modeling (SEM) (McIntosh and Gonzalez-Lima, 1994), Granger causality (Kamiński et al., 2001) and even Graph Neural Networks were recently used for causal modeling (Wein et al., 2021). The above differ based on the assumptions made about the system (Friston, 2003, Lytton, 2008). The SEMs assume that the interactions are linear and the inputs are treated as unknown and stochastic, while DCMs assume that a brain is a deterministic nonlinear dynamic system.

The modeling framework of choice is Causal Bayesian Networks (CBN). It has been widely used in neuroscience for studying multisensory perception (Kording et al., 2007) and functional brain connectivity (Rajapakse and Zhou, 2007).

The application to the iEEG data is motivated by the presence of latent confounders. A confounder is a variable that effects both an assumed cause and an effect, resulting in a spurious association between them. The problem arises from the limited positioning of electrodes, such that it is impossible to observe all the spike sources. The utilized CBN framework can detect the cause-effect relationship in a system with latent confounders (Grosse-Wentrup et al., 2015).

Chapter 3

Dataset description

Intracranial EEG (iEEG) is a method used for the investigation and treatment of various pathological conditions, including drug-resistant epilepsy.

As well as EEG, the iEEG measures voltage fluctuations resulting from ionic current within the neurons of the brain. The intracranial recordings are more valuable in identifying the source of epileptogenic activity since electrodes are located closer to the physiological onset-generating region.

The SEEG recordings were analyzed in this study. The depth electrodes of SEEG measure the local field potential of a neural population in a sphere with a radius of 0.5–3 mm around the tip of a macro-contact (Logothetis, 2003). Every electrode consisted of up to 15 macro-contacts and is schematically visualized in Figure 3.1.

The dataset was collected at the University Clinic Erlangen. It consists of ten patients. The patients were undergoing pre-surgical SEEG monitoring for localization of the epileptogenic region. Nine out of ten patients were put on medication. One patient was put off medication treatment. The average duration of the recordings is 2 hours 9 minutes, with the corresponding average number of marked IEDs being 3050. The number of channels, as well as their location, differ from patient to patient. Every patient was recorded in both sleep and wake states. The detailed dataset description can be seen in Appendix A.1.

The markings are defined as the timestamps of the IEDs detected by an experienced clinician. The format of marking is evt. The model is channel-indifferent, so the markings does not have to provide the information on the channel they have been spotted on. Each timestamp is marked in Time measurement units (Tmu). The signal is recorded in the European Data Format (EDF) format. The electrodes were positioned based on a clinician's assumptions of a potential source location.

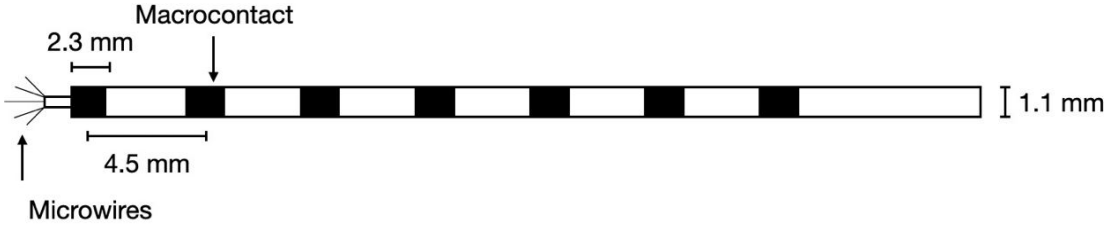

FIGURE 3.1: Sketch of a sample electrode.

Chapter 4

Methodology

The original signal was decomposed into a patient-specific number of components representing different brain activities, including artifacts. A subset of components was chosen based on their average activity during marked IEDs. The resulting components were analyzed for the presence of a causal link between them in form of a chain using the Causal Bayesian Network framework. The resulting causal interactions were recorded, and the distribution of these events corresponding to the time of an IED start was analyzed. Based on the observations, five following hypotheses were stated and tested.

1. H0: number of causal interactions pre-IED = number of causal interactions post-IED
2. H0: number of causal interactions pre-IED = number of causal interactions post-IED in the wake state
3. H0: number of causal interactions pre-IED = number of causal interactions post-IED in the sleep state
4. H0: number of causal interactions post-IED in the sleep state = number of causal interactions post-IED in the wake state
5. H0: number of causal interactions pre-IED in the sleep state = number of causal interactions pre-IED in the wake state

The components that are most frequently a source of causal interactions are assumed to cover the source of epileptogenic activity. The names of channels obtained from the components by inverse decomposition are reported to a clinician. The pipeline of data processing is visible in Figure 4.1.

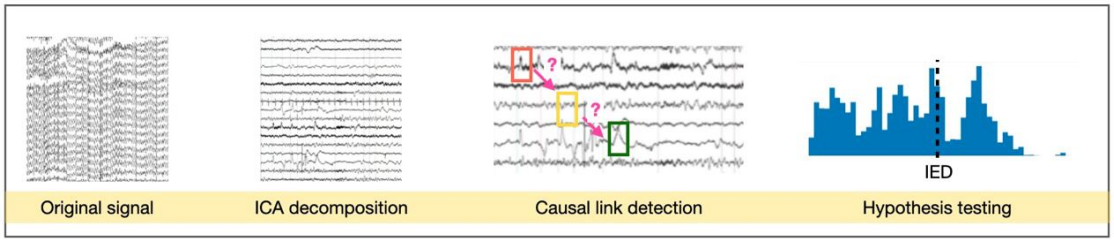

FIGURE 4.1: The pipeline of analysis.

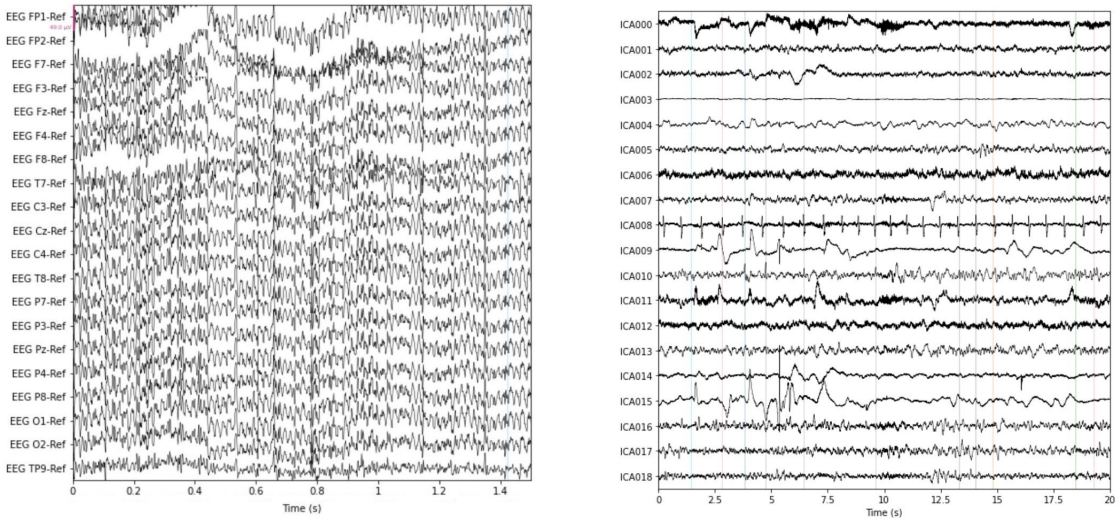

FIGURE 4.2: The original recording of patient №8 (left) and the decomposed independent components (right).

Independent Component Analysis

Independent Component Analysis (ICA), firstly discussed by Herault and Jutten, 1986, is a widely used technique in the signal processing domain. ICA aims to estimate the source signals from a set of recordings where the sources were mixed in unknown ratios.

The easiest way to explain ICA is by bringing up the problem of blind source separation. The three instruments playing in a room are recorded using three microphones. Is it possible to unmix the recordings from three microphones into isolated sounds of every instrument?

The application to SEEG data is similar - a signal consists of k electrodes that are simultaneously recording the electrical activity of a brain. Besides base activity, a signal includes blinks, heartbeats, and muscular activity from swallowing - all recorded simultaneously. The goal is to separate the obtained signal into n independent components that will account for the sources generating these activities. In Figure 4.2, a subset of recorded channels is displayed in the case of patient №8 on the left, and on the right, the corresponding decomposed components are shown. As an example of an artifact, that will be ignored in the further analysis, one can see the heart muscular activity on the component ICA008.

Mathematically, the problem can be formulated as following. Let x represent the recorded signal. The assumption is that x results from mixing the independent sources s by applying a mixing matrix A to them.

$$x = As \tag{4.1}$$

A is an unknown invertible square matrix that mixes the sources. It is the goal of ICA to find the original sources by estimating the unmixing matrix $W = A^{-1}$, such that

$$Wx \approx s \tag{4.2}$$

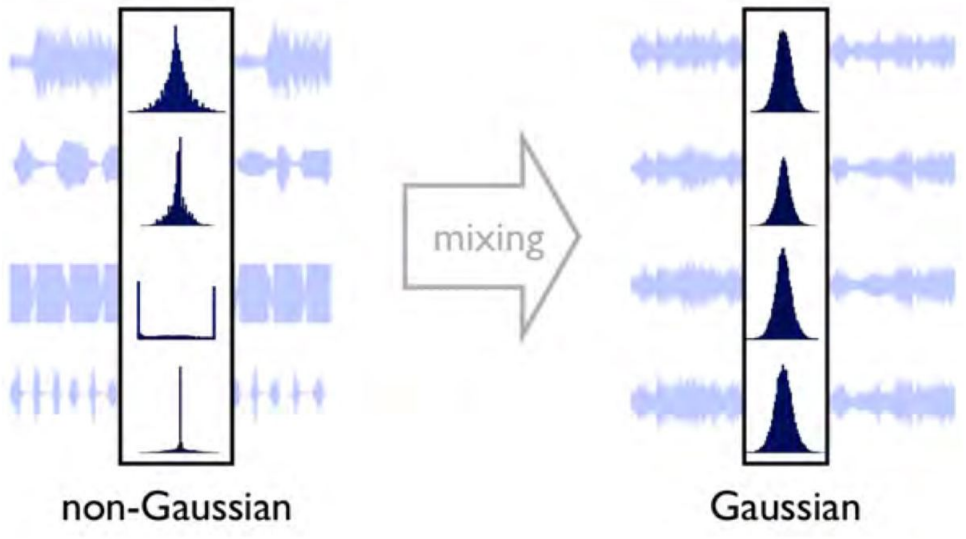

FIGURE 4.3: Comparative distribution of Non-Gaussian sources to the distribution of linear combination of those.

The weights of matrix W are iteratively updated so that the resulting reconstructed sources s either share minimum information (in the case of InfoMax algorithm) or are maximally non-Gaussian (FastICA algorithm).

There are several assumptions that must be met in order to perform ICA decomposition of a signal (Langlois, Chartier, and Gosselin, 2010):

- The sources S_i must be statistically independent.
- The mixing matrix A must be square and full rank. In other words, the number of mixtures must be equal to the number of sources, and the mixtures must be linearly independent of each other.
- The only source of stochasticity in the model is the source s.
- The data is centered.
- The source signals must have a non-Gaussian probability density function except for one single source that can be Gaussian.

The chosen algorithm is FastICA. It approximates the unmixing matrix by maximizing the non-Gaussianity of components. Without the non-Gaussianity assumption, the independent component analysis is not possible at all (Hyvärinen and Oja, 2000). That is nicely illustrated by a Figure 4.3 from Braun, 2020.

The convergence of components $\hat{s}$ to the true sources s using FastICA is guaranteed by the properties of the Central Limit Theorem. The distribution of a sum of independent random variables with finite variance tends towards a Gaussian distribution. In the case of estimation of one component, the reasoning that $\hat{s}$ must be more Gaussian than s is following. The approximation of the true sources, from equation 4.2 is:

$$\hat{s} = Wx \tag{4.3}$$

Let $z = A^T \cdot W$. From the assumptions, A must be square and full rank, thus $W = A^{-1}$ is also square and full rank.

$$\hat{s} = W \cdot x = W \cdot As = (A^T W)^T s = z^T s$$

Since we assume the non-Gaussianity of the sources s, the approximation $\hat{s}$ is more Gaussian than s, and the maximization of the non-Gaussianity of $\hat{s}$ - a linear combination of sources s - will lead to inferring the true sources s. The non-Gaussianily is measured by kurtosis in the used implementation by mne package (Gramfort et al., 2013).

Principal Component Analysis

The number of channels in the original signal is huge and would require a lot of computational resources to perform ICA on. Thus, prior to fitting the FastICA algorithm, the dimensionality of the original matrix x is reduced using Principal Component Analysis. The components of choice should explain at least 95% of the cumulative variance of the data. A benefit of PCA is that the inversely reconstructed signal from the principal components will reduce the initial noise present in the data.

Causal Bayesian Networks

Causal interactions of different brain regions, both prior to and past to occurrence of IEDs was studied using Causal Bayesian Networks (CBN)(Pearl, 2009). A CBN is a graph formed by nodes representing random variables that are connected by links, denoting causal influence. A random variable Y is said to be caused by X if Y depends on X for its value. The causal relations between two components can be expressed visually using directed acyclic graphs (DAGs).

Consider two random variables, X and Y. The cause-effect relationship is inferred from the joint distribution of these two, usually measured by correlation. However, it is not clear whether $X \to Y$ or $Y \to X$.

The cause-effect relation is possible to infer using the notion of Causal Markov Condition (CMC). A node is independent of all variables which are not effects or direct causes of that node, conditional on the set of all its direct causes (Mumford and Ramsey, 2014).

Consider a set of nodes X, Y, and Z.

In case when $P(X|Y) \neq P(X) \to X \not\perp\!\!\!\perp Y$, one can draw an edge between X and Y, depicting the possible relation they hold in a DAG. The same logic can be applied to X and Z and Y and Z. There are three possible graphical models that may arise knowing these dependencies (Figure 4.4): it is not clear what form of dependency they hold: whether they form a chain ($X \to Y \to Z$) (Figure 4.5), a collider ($X \to Y \leftarrow Z$) (Figure 4.7), or a fork ($X \leftarrow Y \to Z$) (Figure 4.6).

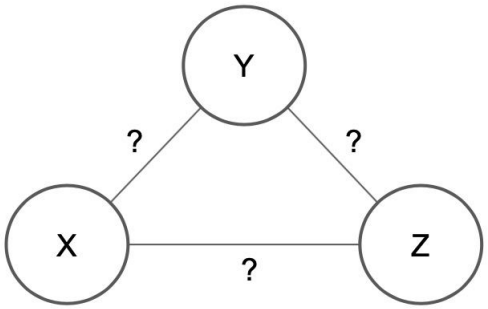

FIGURE 4.4: Undefined graph.

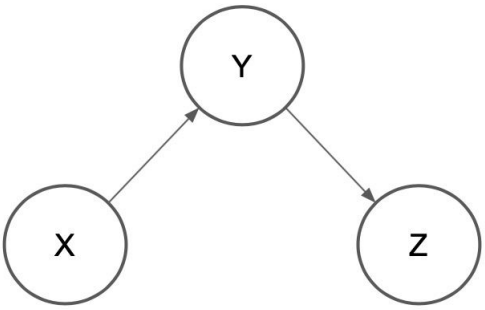

FIGURE 4.5: Chain.

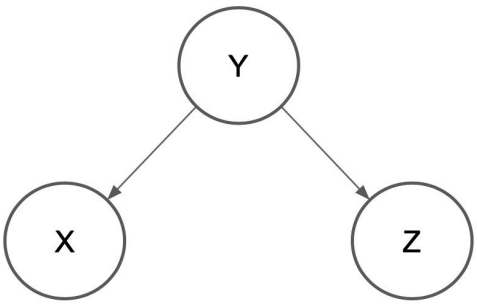

FIGURE 4.6: Fork.

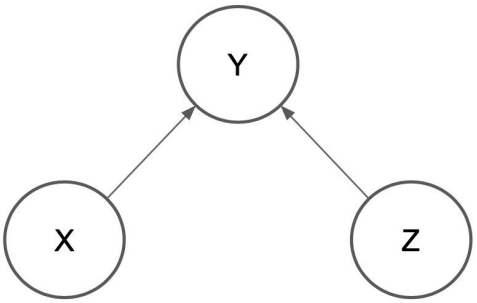

FIGURE 4.7: Collider.

The usage of d-separation can differentiate these cases. Dependency separation, or d-separation, describes the dependence between two nodes or sets of nodes when conditioning on another set of nodes or the empty set. Using CMC, one can connect the joint distribution properties of the variables to their relationship in a DAG.

Thus, if $X \not\perp\!\!\!\perp Y$, but $X \perp\!\!\!\perp Z|Y$, then Y is said to d-separate X and Z.

There are three possible relationships that can arise: chain, fork, and collider. To distinguish between the cases of fork, chain, and collider, one should have a look at conditional distributions of all the pairs of random variables.

A chain is formed if all pairs of variables are dependent Y ans Z ($P(Z = z|Y = y) \neq P(Z = z)$), X and Z ($P(X = x|Z = z) \neq P(X = x)$), and X and Y ($P(X = x|Y = y) \neq P(X = x)$), but are independent given the middle node Y ($P(Z = z|X = x, Y = y) = P(Z = z|Y = y)$).

In the case of fork the following dependencies should be satisfied: X and Y are dependent ($P(Y = y|X = x) \neq P(Y = y)$), Y and Z are dependent ($P(Y = y|Z = z) \neq P(Y = y)$) , Z and X are dependent ($P(Z = z|X = x) \neq P(Z = z)$) , but X and Z are independent conditioned on Y ($P(X = x|Z = z, Y = y) = P(X = x|Y = y)$).

In the case of collider the following dependencies should be satisfied: X and Y are dependent ($P(Y = y|X = x) \neq P(Y = y)$) , Y and Z are dependent ($P(Y = y|Z = z) \neq P(Y = y)$) , Z and X are independent ($P(Z = z|X = x) = P(Z = z)$) , but X and Z are dependent conditioned on Y ($P(X = x|Z = z, Y = y) \neq P(X = x|Z = z)$).

Application

The application of causal analysis to the current task was made to test for a presence of a chain the following hypothesis: whether a brain state at the moment t_0 is a cause of a brain state at time $t_0 + tau$, which causes a state at $t_0 + 2 \cdot tau$. Since not all the components presented abnormal activity during the IEDs, it was inefficient to run the causal analysis algorithm on all the combinations of components by three. Moreover, the components representing artifacts should be removed. Thus, only a subset of components was chosen for the analysis.

A component was chosen based on its activity during IEDs. The ones presenting abnormal behavior were later tested for the presence of a causal relationship. The abnormality was estimated based on the span and deviation of a component during IEDs. An example of all components is visible in Appendix C.1, and the chosen significant components in Appendix C.2.

Every random variable represents a set of values a component takes across all the IEDs on a particular timestamp relative to the start of discharge. A node in a graph is represented by this random variable.

It is best illustrated by an example. Let X be a random variable representing the state of component №1 10 ms before an IED. Then, with a time delay of 0.1 ms, a random variable Y represents a state of component №2 at $10 + 0.1 = 10.1$ ms, and a random variable Z represents a state of component №3 at $10 + 0.1 \cdot 2 = 10.2$ ms. A time delay, denoted as τ, is shifted from 0.1 to the length of the window. An algorithm for causal interaction detection is performed for every combination of all the components by three, forming a chain $ICAX[t_0] \rightarrow ICAY[t_0 + \tau] \rightarrow ICAZ[t_0 + 2 \cdot \tau]$.

Stimulus-based causal inference

In the case of causal analysis on iEGG data the problem of latent confounders arises from the limited positioning of electrodes as well as the number of recording points. Although the epileptic activity is later represented by components, it is impossible to explicitly observe all the sources.

A confounder is a variable that influences both the supposed cause (independent variable) and effect (dependent variables), causing a spurious association between them. An example of a confounding variable can be found in the relationship between alcohol use and lung cancer (Steinke, 2019). The strong association between alcohol use and cancer does not imply a cause-effect relationship between them. The presence of a confounding variable - smoking - affects alcohol consumption because the individuals, who drink often, are more likely to smoke, and the smokers are more likely to get cancer.

The utilized Stimulus-based causal inference (SCI) algorithm was chosen to detect the causal events with the presence of latent confounders (Grosse-Wentrup et al., 2015). The initial brain state at timestamp t_0 is regarded as a stimulus.

A sample test for a chain $X(ICA1[t_0]) \rightarrow Y(ICA2[t_0 + \tau]) \rightarrow Z(ICA3[t_0 + 2 \cdot \tau])$ is conducted as following. Initially, the strength of correlation between

the cause X and the effect Z is measured using correlation coefficient and rejected when the resulting p-value is smaller than significance level α_{rej}. Later, the partial correlation of X and Z conditioned on Y is measured: X and Z are regressed on Y, and the correlation of the residuals e_X and e_Z is recorded. The residuals do not contain the variability in X and Z explained by Y. If the residuals are uncorrelated, one can conclude that $X \perp\!\!\!\perp Z|Y$. Thus, a chain $X \rightarrow Y \rightarrow Z$ is formed. Otherwise, $X \not\perp\!\!\!\perp Z|Y$. The partial correlation measures conditional independence, and if its p-value was lower than significance level α_{acc}, then dependence was rejected.

After a chain is detected, the corresponding starting point of the causal event, along with the time delay and the starting component, are recorded. Out of these causal interactions, a mapping is formed that states the time delay and starting component in correspondence with the number of recorded causal events. The pseudocode for the analysis can be found in Grosse-Wentrup et al., 2015.

Inverse decomposition: component to channel mapping

The original dataset, denoted by a matrix x, is an m by n matrix, where m is the number of original channels and n is the duration of a signal. Later, a linear operator - the unmixing matrix W - is inferred using FastICA and applied to the data to get the independent sources s.

$$s = W \cdot x$$

The decomposed sources s present brain activity on the corresponding components. The source matrix s is a k by n matrix, where k is the number of decomposed components and n is the duration of a signal.

The pseudo-inverse of W is the matrix A - the linear operator that maps independent sources s to the original data x.

$$x = A \cdot s$$

The following intuition was applied to map the chosen components to channels of the original signal. Every independent component is a composition of the original channels. A jth column in the mixing matrix A conveys each original channel's weight forming a component j. Thus, an entry $[i, j]$ of A is a contribution of the jth channel to component i. One can infer the location of a component by analyzing the weight each channel contributes to its composition. A spanned region was proposed based on the weights of channels to a composition of the source components.

When performing a causal analysis, the source component is recorded every time the chain starting on it is detected. The components were sorted by frequency of being source nodes. Later, the top three of them are considered to span a potential IED source. The names of inversely inferred channels are

reported to a clinician at the end of analysis execution and saved into a text file locally.

Chapter 5

Results

Hypothesis testing

After the causal modeling, the distribution of the causal events relative to an IED was analyzed. The averaged results were normalized per patient according to the number of markings for windows 100 and 500 ms. The distributions are visible in Appendix D.1 and D.2.

Figure 5.1 shows the distribution of causal interactions starting at corresponding timestamps relative to an IED along with the activity of chosen components. As assumed, the causal activity is greater before an IED and decreases afterward. The component that has most frequently been detected as a source node of generated activity is ICA010. The channels that put the most weight on the component ICA010 are RTC5-6 and RTB 5-7, visible in Figure 5.2.

The above coincide with the channels of the marked IEDs by a clinician, although the model did not have the information about them.

The results show that the causal activity increases before a discharge and decreases afterward. Based on the observed activity trends, five hypotheses were established :

1. H0: number of causal interactions pre-IED = number of causal interactions post-IED

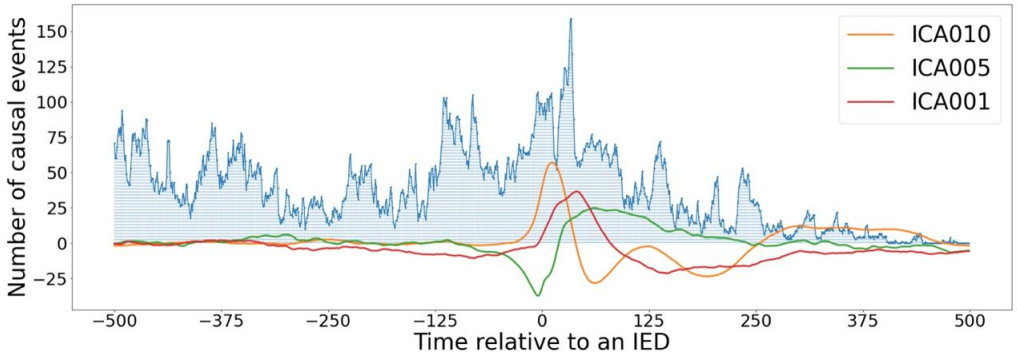

FIGURE 5.1: Number of causal interactions relative to the start of IED vs. averaged component state during the IEDs, patient №10.

Test name	$p_{val}100$	H_0 rejected	$p_{val}500$	H_0 rejected
pre-IED = post-IED	10^{-5}	True	10^{-5}	True
pre-IED in wake = post-IED wake	$2 \cdot 10^{-4}$	True	10^{-5}	True
pre-IED in sleep = post-IED sleep	10^{-5}	True	10^{-5}	True
post-IED in sleep = post-IED wake	0.488	False	10^{-5}	True
pre-IED in sleep = pre-IED wake	0.103	False	10^{-5}	True

TABLE 5.1: Hypothesis testing results: $p_{val}100$ corresponds to the tests on the distributions with a window of length 100 ms and $p_{val}500$ - to those of length 500 ms.

2. H0: number of causal interactions pre-IED = number of causal interactions post-IED in the wake state

3. H0: number of causal interactions pre-IED = number of causal interactions post-IED in the sleep state

4. H0: number of causal interactions post-IED during sleep = number of causal interactions post-IED in the wake state

5. H0: number of causal interactions pre-IED during sleep = number of causal interactions pre-IED in the wake state

The number of causal interactions was collected across all the subjects in wake and sleep states correspondingly.

Firstly, the window of 100 ms preceding and following an IED was analyzed for causal activity. However, the results showed the potential increase in the number of causal interactions starting earlier. That is the reason why the window was extended to half a minute.

The statistical hypothesis test of choice is the permutation test. Permutation tests are non-parametric tests that rely solely on the assumption of exchangeability (Wikipedia contributors, 2022). A test is conducted as follows. The difference in test statistics between the groups is tested for significance using subsampling. In the case of the first hypothesis, the random variable X_A would correspond to number of causal interactions preceding an IED and X_B - to that following an IED. The test statistic of choice in mean. The difference in means from different groups is denoted as T_{obs}. Then, each group was randomly subsampled k times, and the same statistic for a subsample was calculated. As a result of k permutations, we get the sample distribution of the difference in statistics between groups A and B. The one-sided p-value of the test is calculated as the proportion of sampled permutations, where the difference in means is greater than T_{obs}. For a significance level α, in case when T_{obs} is not contained within $(1 - \alpha) \times 100\%$ of recorded differences,the H_0 was rejected and H_1 was accepted, stating that the statistics differ across the groups.

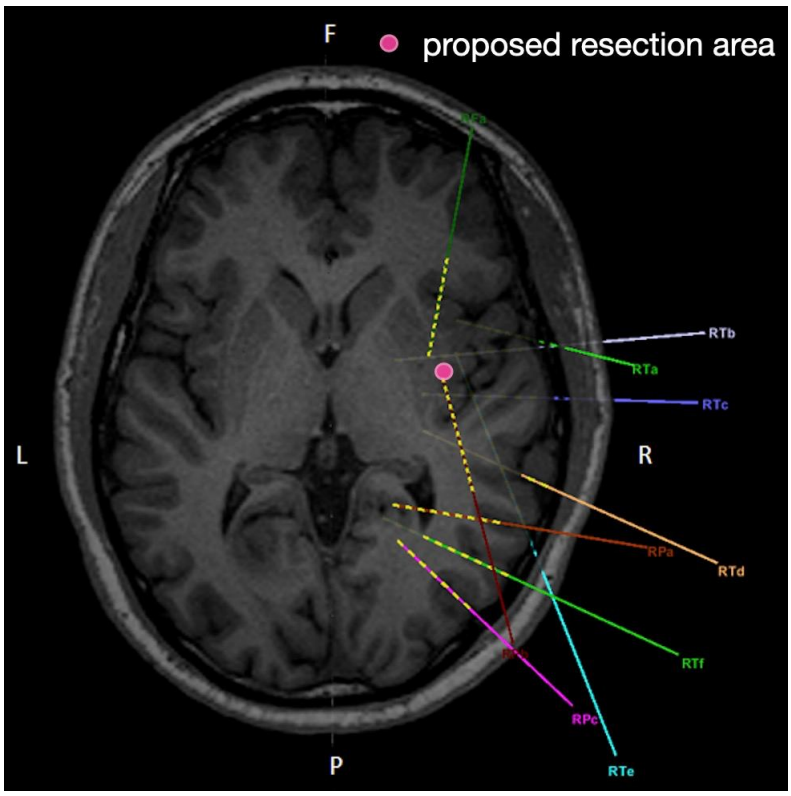

FIGURE 5.2: Proposed resection area in case of patient №8.

Epileptogenic region localization

The resection area was later compared to the reported source of causal activity. For each component, the five channels with the biggest weight were chosen. The proposed onset-generating area in the case of patient №8 is visible in Figure 5.2, and the results of the same analysis in patients №1 and 10 are visible in Appendix B.

The results on proposed channels were consistent across different windows of analysis. Moreover, the model is did not take into consideration the channels where the markings were detected. Nevertheless, the channels obtained by the inverse decomposition coincided with the ones considered as significant by a clinician.

Chapter 6

Conclusion

The results of the study can be applied and developed in different directions. The noted increase of interactions before an IED can be used for predictability of discharges. The results showed a statistical difference between the causal activity preceding and following an IED, as well as across awareness states.

The second benefit is a computer assistant for a clinician during the detection of the epileptogenic region. The obtained channels will shade a light onto the potential resection area supporting a clinician during diagnosing. One of the consequences of the proposed area localization is potential reduction of the resection region.

Limitations

The data of a patient are hard to obtain, and the time required for a clinician to label the IEDs is of high value. The number of possible combinations of chosen components was enormous. Thus, an experiment could last up to a week in some cases.

Further steps

For the evaluation of the model's accuracy, the correct determination of the epileptogenic region in 3D must be defined and later compared to the true removed area. The reported recurrence of seizures after the resection will evaluate the effectiveness of estimations. Another investigation track would be analyzing causal activity with a longer window, as the activity trends did not show their start 500 ms before an IED.

Appendix A

TABLE A.1: Dataset description.

Patient №	Channels №	State	Duration, minutes	Markings №
1	148	sleep wake	112 115	2602 7009
2	128	sleep wake	132 132	1664 1709
3	101	sleep wake	168 168	711 1283
4	131	sleep wake	130 130	11269 486
5	162	sleep wake	105 105	765 2722
6	109	sleep wake	156 156	819 289
7	145	sleep wake	117 22	2235 1533
8	124	sleep wake	137 137	1997 356
9	111	sleep wake	153 153	652 530
10	138	sleep wake	123 122	5728 5084

Appendix B

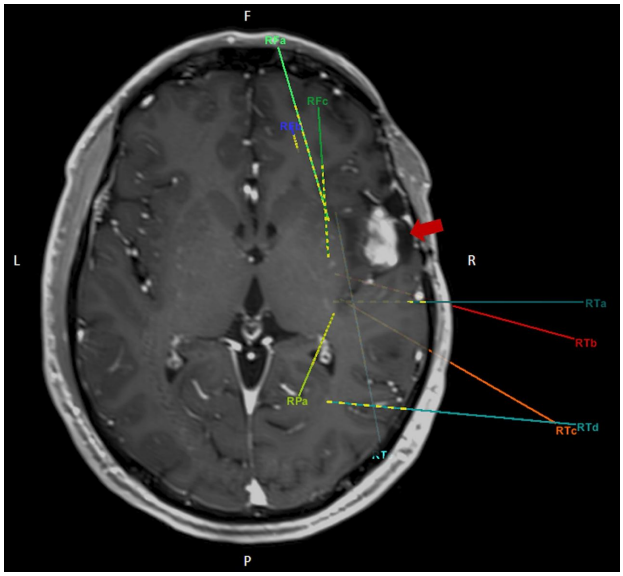

FIGURE B.1: MRI based 3D scheme of SEEG implantation: patient № 10.

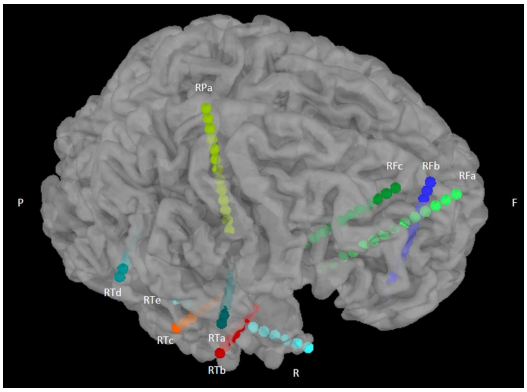

FIGURE B.2: Cortical reconstruction from MRI of the patient №10.

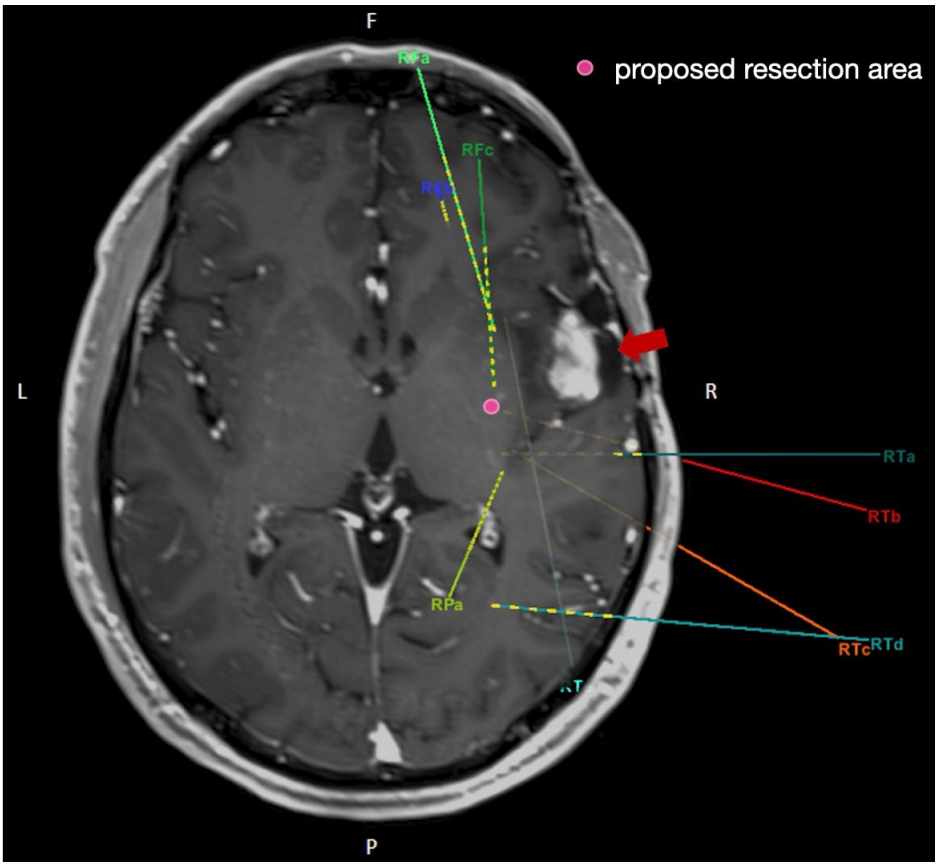

FIGURE B.3: Proposed resection area in case of patient №10.

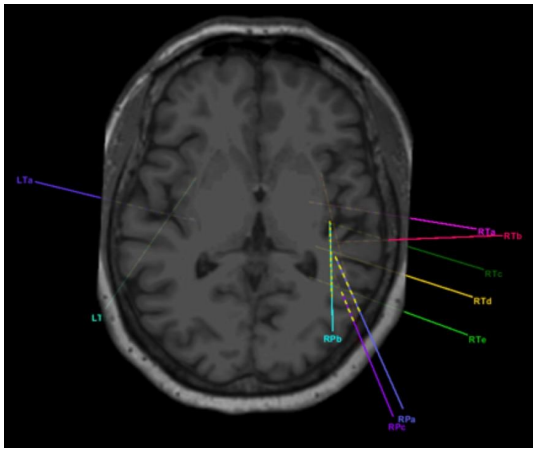

FIGURE B.4: MRI-based 3D scheme of SEEG implantation: patient № 1.

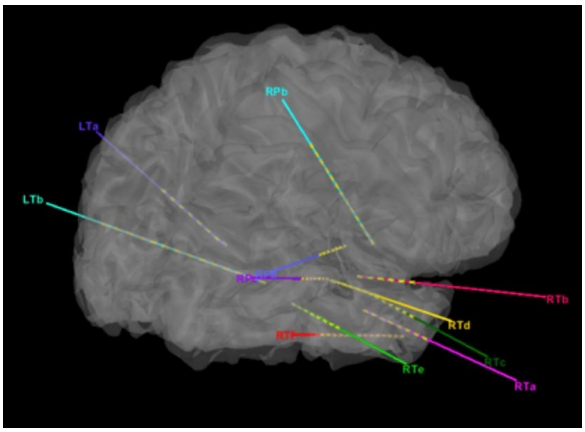

FIGURE B.5: Cortical reconstruction from MRI of the patient №1.

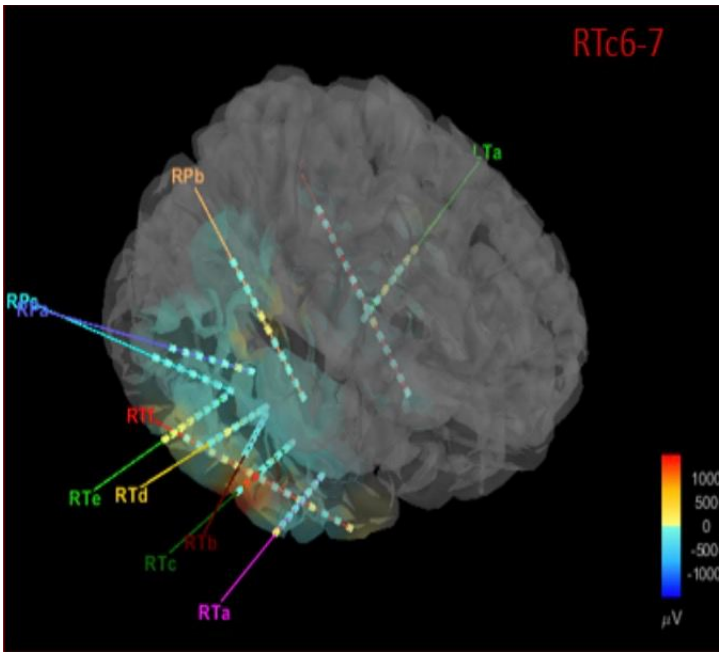

FIGURE B.6: The area of most frequent IEDs marked by a clinician, patient №1.

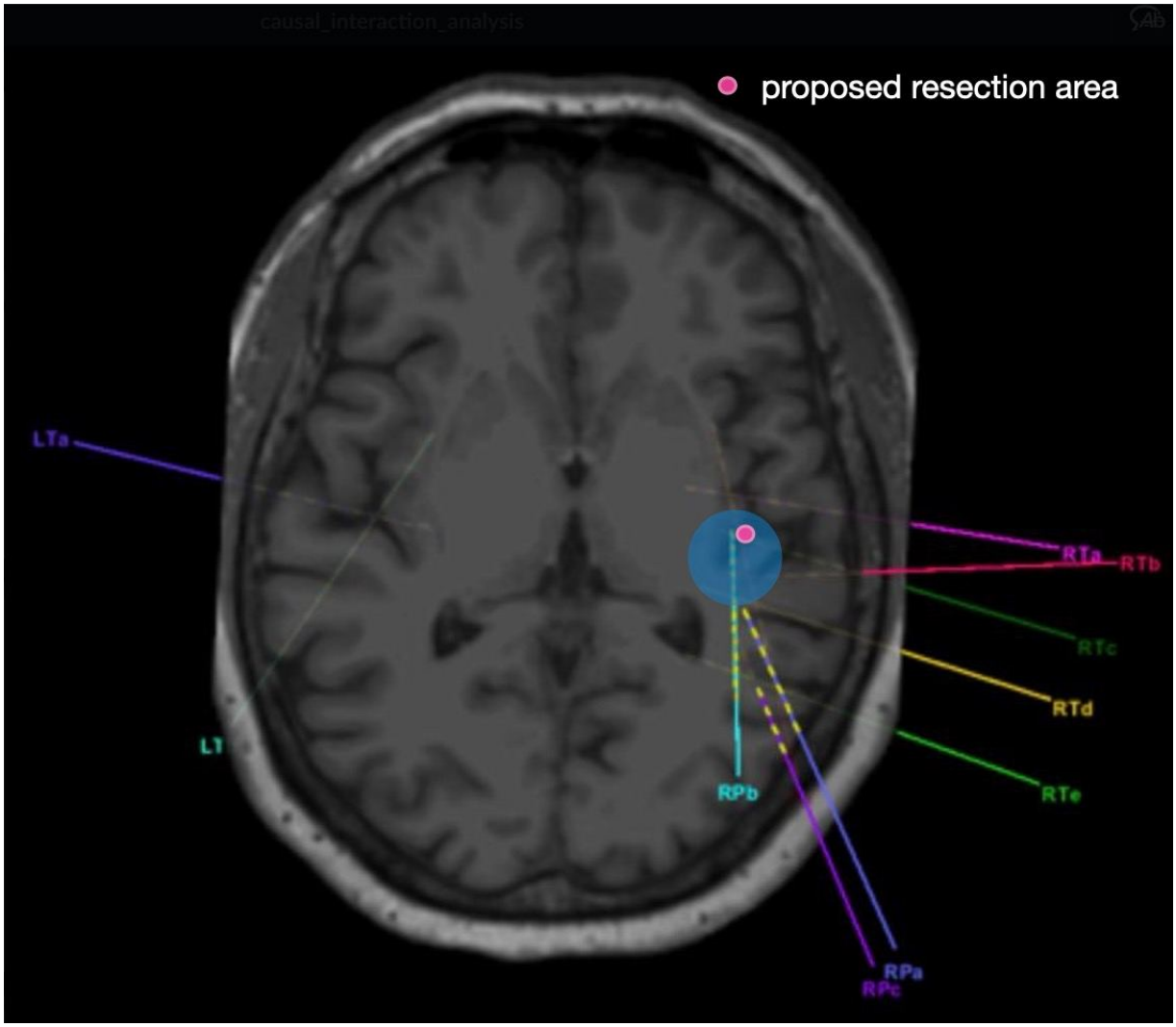

FIGURE B.7: The area of most frequent IEDs proposed by an algorithm, patient №1.

Appendix C

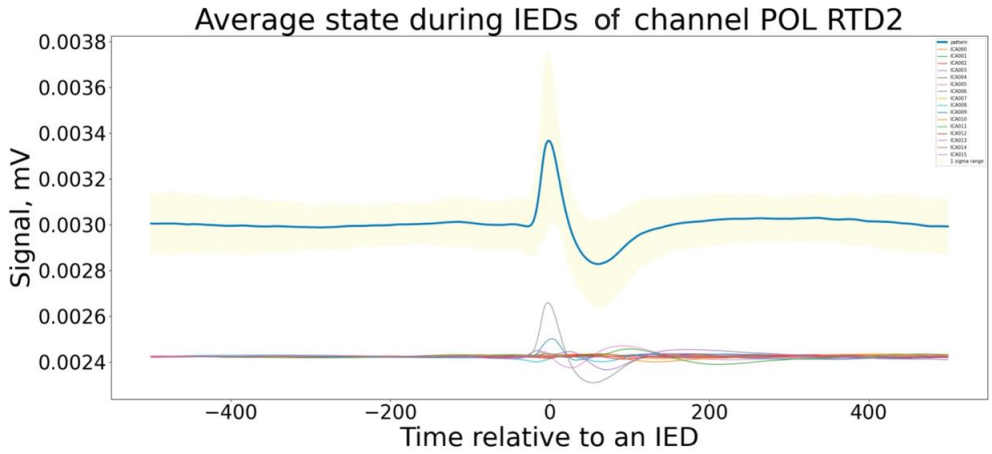

FIGURE C.1: Averaged state of all the components during all the IEDs along with the averaged state of channel POL RTD2 during all the IEDs. Patient №8.

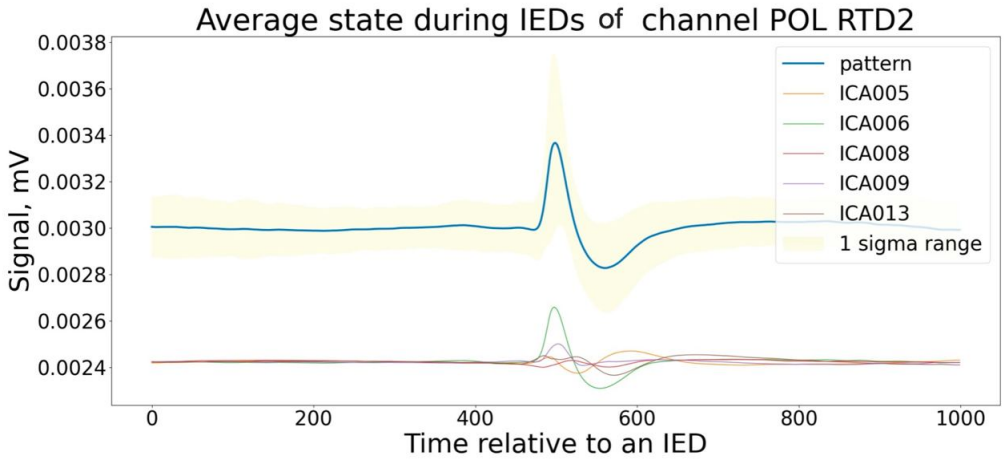

FIGURE C.2: Averaged state of chosen significant components during all the IEDs along with the averaged state of channel POL RTD2 during all the IEDs. Patient №8.

Appendix D

The following is the averaged distribution of causal activity across all the patients. The number of detected interactions was normalized by the number of markings for every patient individually. The normalization step reasoning is that the larger the number of markings, the bigger the probability of detecting an interaction. Thus, a patient with 2602 markings could have prevailed over a patient with 530 markings skewing the distribution and making it non-representative. The y axis could not be interpreted as a number of causal interactions, so it was removed.

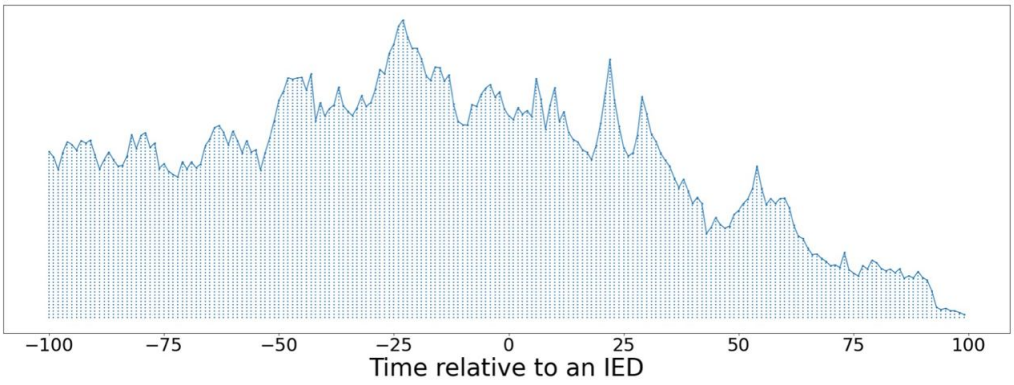

FIGURE D.1: Averaged and normalized distribution of causal interactions relative to the beginning of a chain: 100 ms.

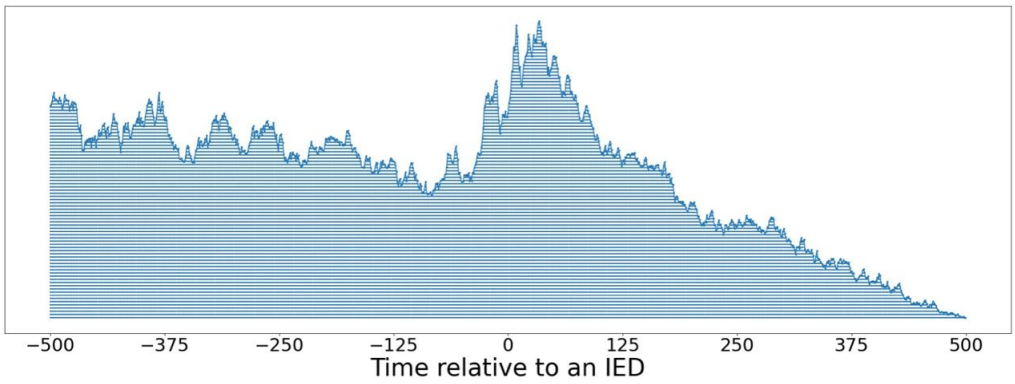

FIGURE D.2: Averaged and normalized distribution of causal interactions relative to the beginning of a chain: 500 ms.

Bibliography

Alarcon, G et al. (1997). "Origin and propagation of interictal discharges in the acute electrocorticogram. Implications for pathophysiology and surgical treatment of temporal lobe epilepsy". In: *Brain* 120 (12), 2259–2282. DOI: 10.1093/brain/120.12.2259.

Amini, Ladan et al. (2011). "Directed Differential Connectivity Graph of Interictal Epileptiform Discharges". In: *IEEE Transactions on Biomedical Engineering* 58, pp. 884–893.

Azeem, Abdullah et al. (May 2021). "Interictal spike networks predict surgical outcome in patients with drug-resistant focal epilepsy". In: *Annals of clinical and translational neurology* 8. DOI: 10.1002/acn3.51337.

Bartolomei, Fabrice et al. (2016). "What is the concordance between the seizure onset zone and the irritative zone? A SEEG quantified study". In: *Clinical Neurophysiology* 127.2, pp. 1157–1162. ISSN: 1388-2457. DOI: https://doi.org/10.1016/j.clinph.2015.10.029. URL: https://www.sciencedirect.com/science/article/pii/S1388245715009827.

Biswas, Rahul and Eli Shlizerman (2022). "Statistical Perspective on Functional and Causal Neural Connectomics: A Comparative Study". In: *Frontiers in Systems Neuroscience* 16. DOI: 10.3389/fnsys.2022.817962.

Braun, Jochen (2020). *ICA*. https://bernstein-network.de/wp-content/uploads/2021/03/Lecture-16-Independent-component-analysis-2020.pdf. Accessed: 2022-05-20.

Cohen, Michael (Jan. 2014). *Analyzing Neural Time Series Data: Theory and Practice*, pp. 31–34. ISBN: 9780262319553. DOI: 10.7551/mitpress/9609.001.0001.

Engel, Jerome et al. (Mar. 2012). "Early Surgical Therapy for Drug-Resistant Temporal Lobe Epilepsy A Randomized Trial". In: *JAMA : the journal of the American Medical Association* 307, pp. 922–30. DOI: 10.1001/jama.2012.220.

Epilepsy, Society (2021). *Epilepsy Surgery*. https://epilepsysociety.org.uk/about-epilepsy/treatment/epilepsy-and-brain-surgery. Accessed: 2022-05-16.

Friston, K. (Dec. 2003). "Dynamic Causal Modelling". In: vol. 19, pp. 1063–1090. DOI: 10.1016/B978-012264841-0/50054-8.

Friston, Karl (Dec. 2008). "Hierarchical Models in the Brain". In: *PLoS computational biology* 4, e1000211. DOI: 10.1371/journal.pcbi.1000211.

Gotman, Jean (1991). "Relationships Between Interictal Spiking and Seizures: Human and Experimental Evidence". In: *Canadian Journal of Neurological Sciences / Journal Canadien des Sciences Neurologiques* 18.S4, 573–576. DOI: 10.1017/S031716710003273X.

Gramfort, Alexandre et al. (2013). "MEG and EEG Data Analysis with MNE-Python". In: *Frontiers in Neuroscience* 7.267, pp. 1–13. DOI: 10.3389/fnins.2013.00267.

Grosse-Wentrup, Moritz et al. (Oct. 2015). "Identification of causal relations in neuroimaging data with latent confounders: An instrumental variable approach". In: *NeuroImage* 125. DOI: 10.1016/j.neuroimage.2015.10.062.

Health NIH, National Institutes of (July 2009). *Human Connectome Project*. https://www.nih.gov/news-events/news-releases/nih-launches-human-connectome-project-unravel-brains-connections. Accessed: 2022-05-23.

Herault, J. and C. Jutten (Aug. 1986). "Space or time adaptive signal processing by neural network models". In: *Neural Networks for Computing*. Vol. 151. American Institute of Physics Conference Series, pp. 206–211. DOI: 10.1063/1.36258.

Hyvärinen, A. and E. Oja (2000). "Independent component analysis: algorithms and applications". In: *Neural Networks* 13.4, pp. 411–430. ISSN: 0893-6080. DOI: https://doi.org/10.1016/S0893-6080(00)00026-5. URL: https://www.sciencedirect.com/science/article/pii/S0893608000000265.

Kamiński, MJ et al. (Sept. 2001). "Evaluating causal relations in neural systems: Granger causality, directed transfer function and statistical assessment of significance". In: *Biological cybernetics* 85, pp. 145–57. DOI: 10.1007/s004220000235.

Kiriakopoulos, Elaine (Oct. 2019). *Understanding Seizures*. https://www.epilepsy.com/what-is-epilepsy/understanding-seizures. Accessed: 2022-05-16.

Kording, Konrad et al. (Sept. 2007). "Causal Inference in Multisensory Perception". In: *PloS one* 2, e943. DOI: 10.1371/journal.pone.0000943.

Langlois, Dominic, Sylvain Chartier, and Dominique Gosselin (2010). "An Introduction to Independent Component Analysis: InfoMax and FastICA algorithms". In: *Tutorials in Quantitative Methods for Psychology* 6.1, pp. 31–38. DOI: 10.20982/tqmp.06.1.p031. URL: http://www.tqmp.org/RegularArticles/vol06-1/p031/p031.pdf.

Logothetis, Nikos (June 2003). "The Underpinnings of the BOLD Functional Magnetic Resonance Imaging Signal". In: *J Neurosci* 23, pp. 3963–71. DOI: 10.1523/JNEUROSCI.23-10-03963.2003.

Lytton, William (Sept. 2008). "Computer modeling of Epilepsy". In: *Nature reviews. Neuroscience* 9, pp. 626–37. DOI: 10.1038/nrn2416.

McIntosh, A. and F. Gonzalez-Lima (Jan. 1994). "Structural equation modeling and its application to network analysis in functional brain imaging". In: *Human Brain Mapping* 2, pp. 2–22. DOI: 10.1002/hbm.460020104.

Mumford, Jeanette A. and Joseph D. Ramsey (2014). "Bayesian networks for fMRI: A primer". In: *NeuroImage* 86, pp. 573–582. ISSN: 1053-8119. DOI: https://doi.org/10.1016/j.neuroimage.2013.10.020. URL: https://www.sciencedirect.com/science/article/pii/S1053811913010392.

Pearl, Judea (Jan. 2009). "Causal Inference in Statistics: An Overview". In: *Statistics Surveys* 3, pp. 96–146. DOI: 10.1214/09-SS057.

Picot, Marie-Christine et al. (2008). "The prevalence of epilepsy and pharmacoresistant epilepsy in adults: a population-based study in a Western European country". In: *Epilepsia* 47 (7), pp. 1230–1238.

Qi, Lei et al. (2020). "Identifying the Epileptogenic Zone With the Relative Strength of High-Frequency Oscillation: A Stereoelectroencephalography Study". In: *Frontiers in Human Neuroscience* 14. ISSN: 1662-5161. DOI: 10.3389/fnhum.2020.00186. URL: https://www.frontiersin.org/article/10.3389/fnhum.2020.00186.

Rajapakse, Jagath and Juan Zhou (Oct. 2007). "Learning effective brain connectivity with dynamic Bayesian networks". In: *NeuroImage* 37, pp. 749–60. DOI: 10.1016/j.neuroimage.2007.06.003.

Steinke, Douglas T. (2019). "Chapter 14 - Essentials of Pharmacoepidemiology". In: *Clinical Pharmacy Education, Practice and Research*. Ed. by Dixon Thomas. Elsevier, pp. 203–214. ISBN: 978-0-12-814276-9. DOI: https://doi.org/10.1016/B978-0-12-814276-9.00014-3. URL: https://www.sciencedirect.com/science/article/pii/B9780128142769000143.

Wein, Simon et al. (Apr. 2021). "A graph neural network framework for causal inference in brain networks". In: *Scientific Reports* 11. DOI: 10.1038/s41598-021-87411-8.

WHO, World Health Organization (Feb. 2022). *Epilepsy*. https://www.who.int/news-room/fact-sheets/detail/epilepsy. Accessed: 2022-05-16.

Wikipedia contributors (2022). *Permutation test — Wikipedia, The Free Encyclopedia*. [Online; accessed 1-June-2022]. URL: https://en.wikipedia.org/w/index.php?title=Permutation_test&oldid=1087443797.